SYNTHESIS REPORT
FOR PUBLICATION

CONTRACT N" : BREU CT 91 0518 (RZIE)

PROJECT No : P 4096-90

ITITLE :

LASER WELDING OF SUPERALLOYS
AND OF TITANIUM ALLOYS

PROJECT
COORDINATOR: R.T.M. S.p.A. Istituto per le Ricerche di Tecnologia
Meccanica e per 1' Automazione
10080 - VICO CANAVESE - TORINO - ITALY
Tel.+39 125 7472516/7; Fax :+39 125 74755;
E mail rtm@rtm.it

PARTNERS :

- **MTU-Motoren Turbinen Union -Daimler Benz Aerospace; München (DE).**
- **Snecma - Société Nationale d'Etúdes et de Construction de Moteurs d' Avion; Evry Corbeil (FR).**
- **. Alfa Romeo Avio - Società Aeromotoristica per Azioni ; Pomigliano (IT).**
- **Aerospatiale -Centre de Recherche L. Bleriot; Suesnes (FR).**
- **. Lumonics - Lasers - Swift Valley, Rugby (GB)**
- **. Cetim - Centre Technique de l'Industrie Mechanique Française; Senlis (FR).**

STARTING DATE : 01/02/ 1992 **DURATION : 48 Months**

PROJECT FUNDED BY THE EUROPEAN COMMUNITY UNDER THE . . BRITE / EURAM PROGRAMME.

DATE: SEPTEMBER, 1996

LASER WELDING OF SUPERALLOYS AND OF TITANIUM ALLOYS

S, *L.Gobbi,* - RTM. Istituto per le Ricerche di Tecnologia Meccanica c per I' Automatione; 10080 Vito Canavese, *Li Zhang* Torino, Italy; Project *Coordination.* Fax + 3912574755, Tel, +39 12574725, E - mail rtm@rtm.it
K. I-J. Richter -Motoren und Turbinen Union (MTU) GmbH. Daimler Benz Aerospace; Dachauerstrasse 665, D 8000, Munchen (DE).
R. Festa -Alfa Romeo Avio. Società Aeromotoristica per Azioni; Viale Impero, 80038 Pomigliano, Napoli, (IT).
J. Y. Loreau, -Snecma; Sociètè Nationale d' Etude et de Construction de Moteurs d' Avion: BP 81, RN 7, 91003,
M.Allovard Evry Cedex (FR).
J.F.Ramiere -Aerospatiale, Centre Commun dc Recherches Louis Bleriot: 12 Ruc Pasteur. 92152 Suresnes Cedex (FR).
I . Norris -Lumonics LTD; Cosford Lane,. Swift Valley, Rugby. CV21 1 QN. (GB).
J. F.Flavenot, -Cetim, Centre Tecnique de l'Industrie Mecanique Française; 52 Av. Félix Louat, BP 67.60304.
P. Merrien Senlis cedes (FR).

ABSTRACT

Description is given of the basic research in the welding of the most widely used superalloys and of titanium alloys as well as of the representative components of power plants and crafts used in aeronautic. space and other industrial applications having thickness ranging from 0.S to 13 mm. CO_2 lasers up to 13 kW and solid state Nd:YAG ones up to the experimental 6 kW arc available within the partnership. The metallurgy of Inconel 718 related to the Niobium carbides (NbC) and the Delta phase at grain boundaries. consequent to the 10.000 °K/s cooling speed of the fusion zone, is investigated using scanning and transmission electron microscopes. Microfissures free weld were achieved in the annealed state with grain size ASTM 10 or finer. The eutectic of y / Laves was restrained by rapid solidification. Many Delta phases precipitates at interdendrites with 960 'C post weld solution treatment. Above 1038 "C the Laves phase dissolves completely and only NbC is present.
Examples of smooth weld beads suitable for Titanium parts subject to high surface aerodinamical requirements obtained by cosmetic runs are illustrated. Laser cutting and rewelding techniques have been adopted to simplify. speed up and reduce costs in the manufacturing and in the overhauling of lightweight structures, with minimum deformations also making use of optical fibres for complex or hidden parts to be welded. The joints were assessed by residual stress measurements and by Low Cycle Fatigue tests at room and high temperature.

Keywords: Laser welding , Superalloys, Titanium alloy.

1. INTRODUCTION

Over the last 20 years, the operating temperature of jet engines has gradually increased by some 15 'C per year, from 1050 to 1350 'C. This increase improves specific consumption and thrust/weight ratio, but makes design of turbine engines very difficult. Apart from progress made in materials, special shapes are used with carefully designed cavities to achieve efficient cooling, e.g., contra-flow cooled chambers, multi-perforated heat barriers and combustion chambers. The harsh operating conditions mean it is necessary to use superalloy (Fig. 1), which owe their creeps strength to the precipitation of the intermetallic compound carbides in solid solution. This is obtained by quenching followed by ageing. Molybdenum, tungsten, vanadium, niobium. titanium and aluminium are the elements forming the intermetallic compounds.
Titanium alloys. such as Ti6Al4V (6% Al, 4% V), Ti6242 (6% AI. 2% Sn. 4% Zr, 2% Mo) and TiCu2 (2% Cu) arc widely used in aeronautic and aerospace structures e.g. blades and casings of compressor stages in turbojets. Tungsten Inert Gas (TIG) and Electron Beam (EB) are the most widespread techniques for welding the above alloys [2.3,4], However, lasers can be a convenient alternative for welding even complex-shaped components made of these alloys with the following aims:
-meeting industrial requirements for welding, with minimal deformation of workpieces
-welding dissimilar superalloys
-reducing the need for heavy fixtures which arc necessary when conventional high-energy processes are used
-exploiting the potential for organisational streamlining and consequent reduction of floor-to-floor production time of components. which lasers have already made possible in other sectors
-taking advantage of the use of fibre optics to weld complex or hidden parts
-performing the operations of cutting and cutting plus rewelding on the same station, for use both in manufacture of new structures and overhauling of worn-off ones
-assessing the feasibility of new designs for industrial products with fewer parts requiring assembly, where laser technology can be incorporated right from the design stage.

2 . BASIC INVESTIGATIONS ON *THE* TECHNIQUE *AND THE METALLURGY IN SUPERALLOYS LASER WELDING, WITH PARTICULAR REGARD TO WROUGHT INCONEL* 718.

Because of its excellent resistance to post welding heat treatment cracking, the Inconel 718 stands out as the most dominant alloy among many nickel base superalloys, and is extensively used in the aeronautical industry [1,2]. Laser welding, as an advanced technique, required increasingly more research to manufacture aeroengine components. Since Inconel 718 can be susceptible to microfissuring in the heat affected zone (HAZ) much attention has been paid to the mechanism and to the solutions [3,4]: the plasma plume generated by the interaction of power beam on the surface of the materials, results in a nailhead where microfissures frequently occur [5,6] and consequently the fatigue properties are degraded [7]. The main purpose of this

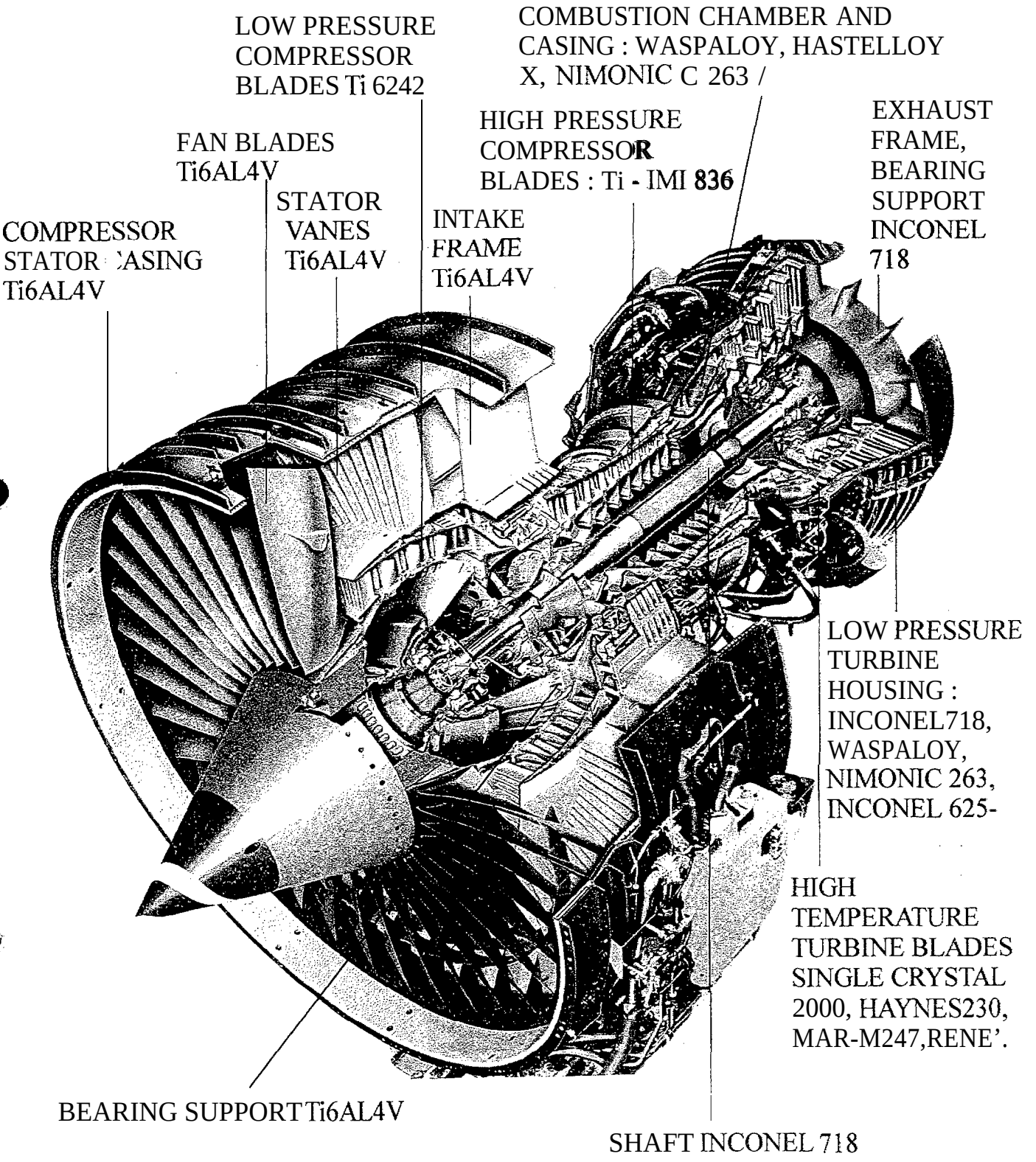

Section of recent turbofan aeroengine where titanium alloys are widely adopted for the compression stages and superalloy for the high temperature combustion/turbine stages.

880 W, 110 mrn/min, f=+.5; 895W, 145, f=+1; 895 W, 145. f=+0.5; 895 W, 160, f=+0.5

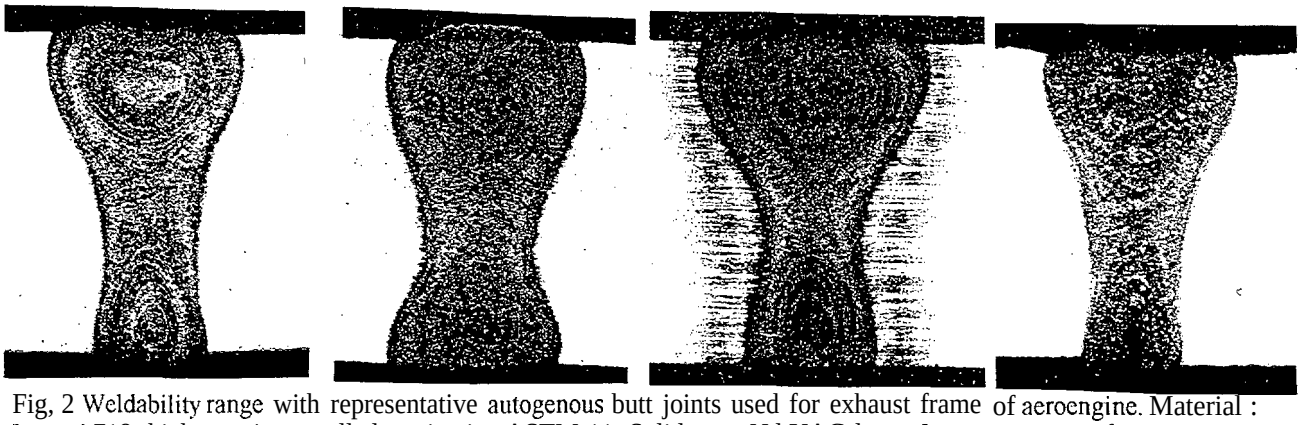

Fig, 2 Weldability range with representative autogenous butt joints used for exhaust frame of aeroengine. Material : Inconel 718 thickness 4mm, rolled. grain size ASTM 11. Solid state Nd:YAG laser, Lumonics JK706 frequency 33 Hz.

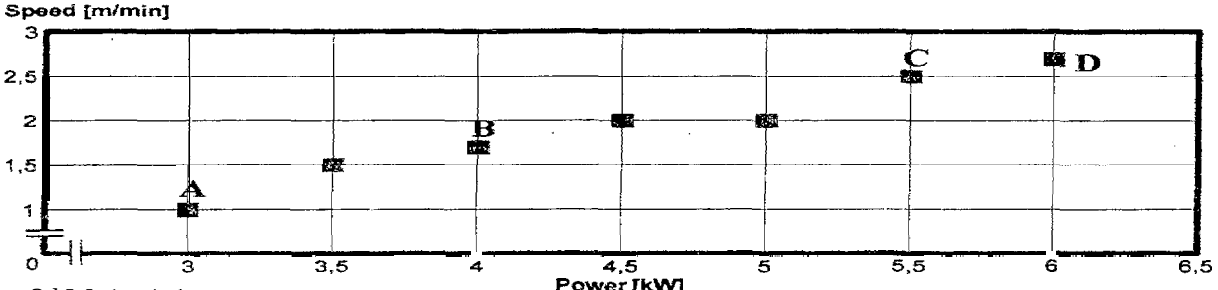

A= 3 kW, 1 m/min B= 4 kW, 1.7 m/min C=5.5 kW, 2,5 m/min D= 6 kW, 2.7. m/min

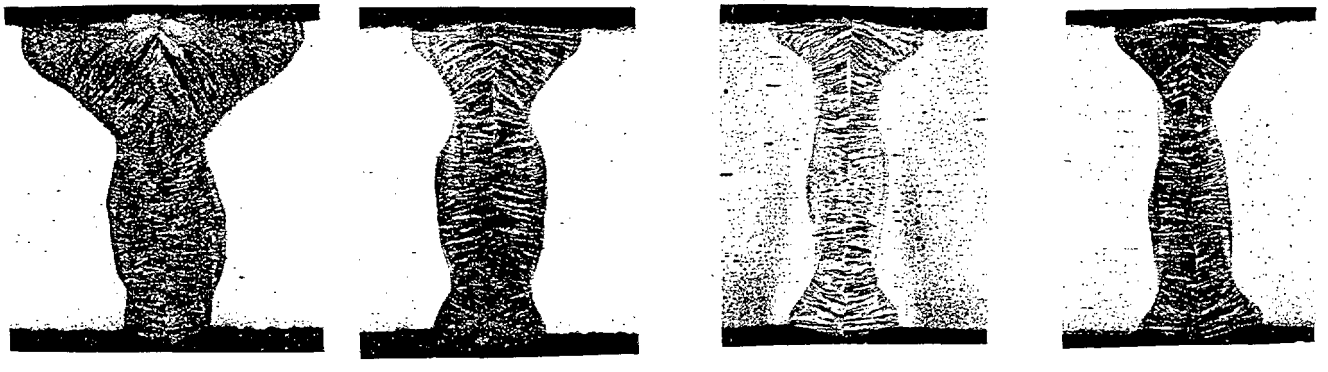

Fig. 3 Weldability range with significative autogenous butt joints used for exhaust frame of aeroengine. Material: Inconel 718 thickness 4 mm, rolled, grain size ASTM 11, Rofin Sinar RS 6000 6kW C02 laser, Focusing mirror 5".

research is to investigate some laser welding techniques in order to obtain sound weldments of industrial parts and better understand the mechanism of microfissuring from real phenomena rather than by simulant tests. The solidified weld microstructures were also revealed, and gave the basic information for the development of the most adequate post welding heat treatments.

The materials used in this study were hot rolled sheet products 8, 6.5 and 4 mm thick. The chemical composition is given in table I. The microstructure of base material will be indicated for each case.

Tab. I Chemical composition of Inconel 718

Ni = Bal	Cr 18,33	Fe 18.01	Nb 5.22
Mo 3	Co 0.46	Mn 0.21	Ti 1.07
Al 0.54	Cu 0.05	Si 0.11	B 0.004
C 0.05	P 0.006	s 0.002	Ag 0.0002
Bi 0.00003	Pb 0.0005		

The partners provided the following equipment:

- $C0_2$ laser from 1 up to 15 kW: Rofin Sinar, Wegman Baasel, Trumpf and Avco Everett.
- Nd:YAG Lumonics lasers from 500 W up to the experimental 6 kW and the 1kW from Quantel.

The microanalysis were performed using Transmission Electron Microscope (TEM), Scanning Electron Microscope (SEM) equipped with Electron Probe Microanalysis (EPMA) and optical microscopes.

The weldability ranges of optimised joints were obtained in the first half of the project for each one of the materials corresponding to the industrial components, which were subsequently welded in the second phase of the project. The optimisation was referred to the internal / international standards currently adopted by the End Users in the project. The power-speed ranges will support the End-Users in making decision about the convenience of the technology. Some of the most significant examples of autogenous butt welds on Inconel 718 using lasers, are given as follows:

- Fig 2, pulsed 1 kW Nd:YAG with optical fibre, on 4 mm in thickness which is close to the limits for the

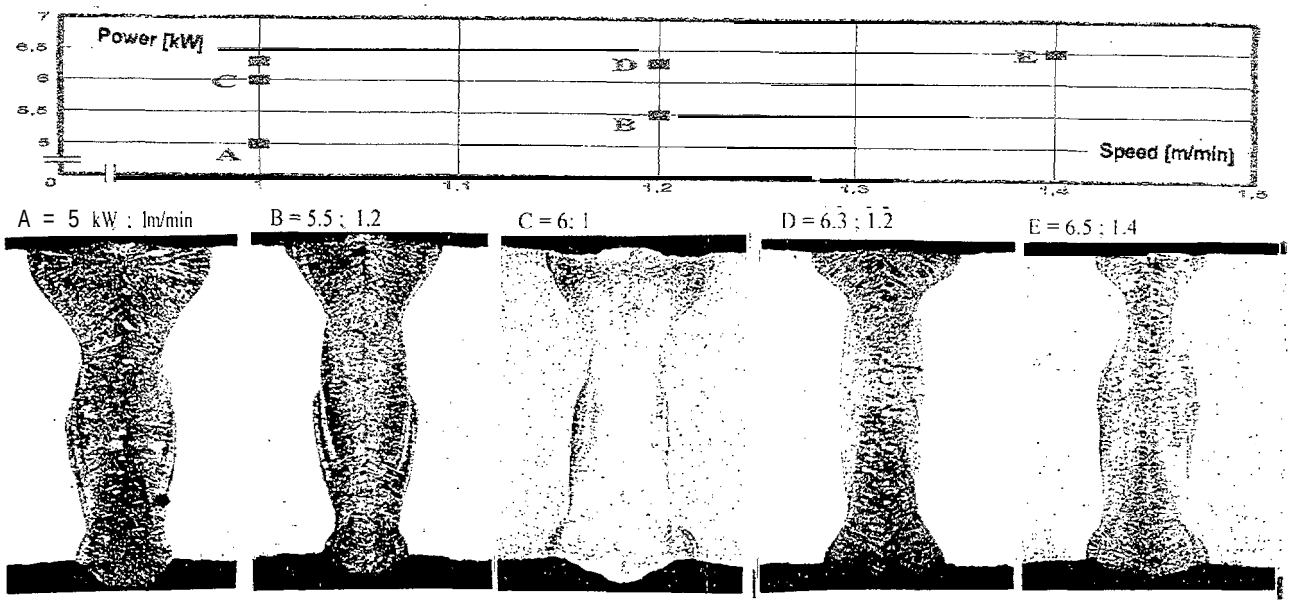

Fig. 4 Weldability range with autogenous butt joints. Material Inconel 718. thickness 6,5 **mm.** rolled, grain size ASTM 11. Rofin Sinar RS 6000 CO_2 laser. Focusing mirror 5".

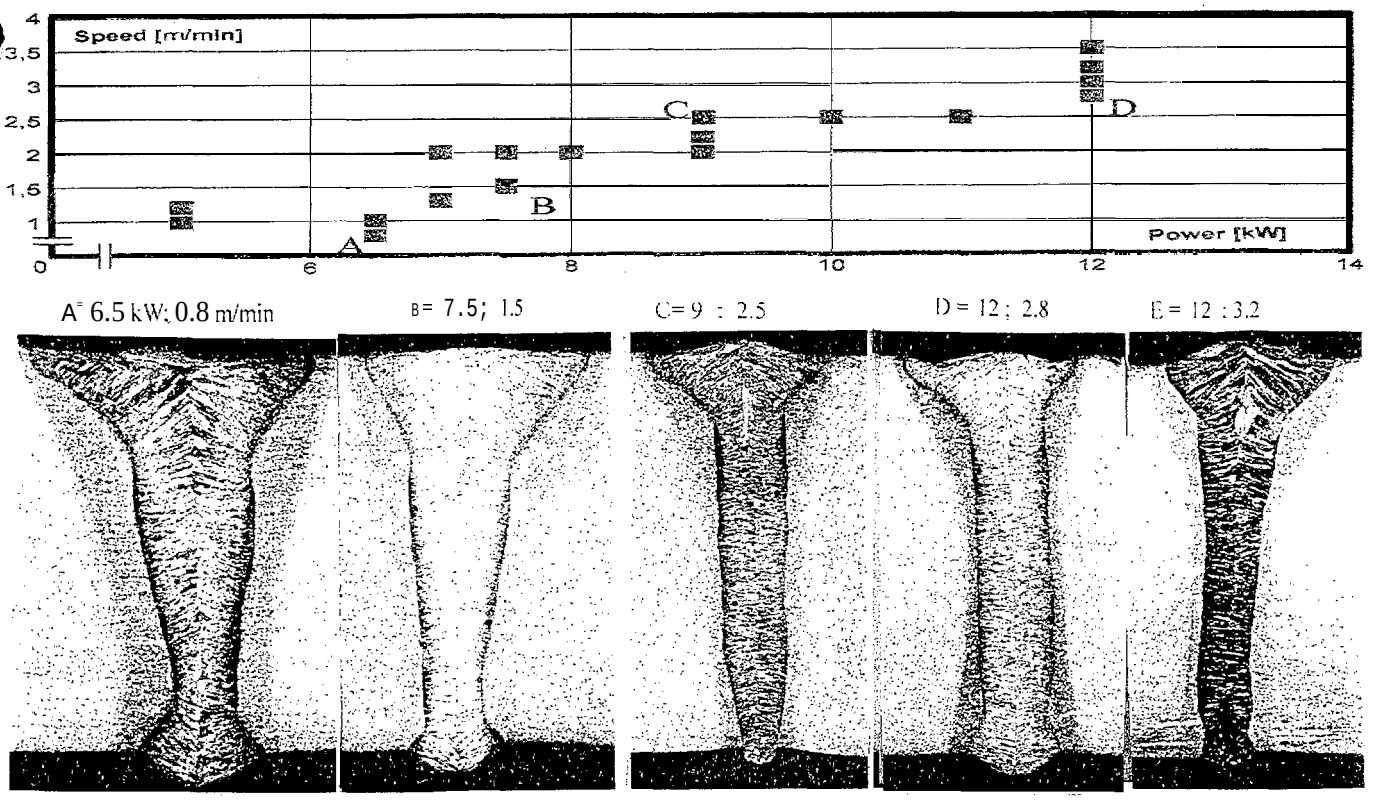

Fig. 5 Weldability range with autogenous butt joints for low pressure turbine housing. Material: Inconel 718, thickness 8 mm, rolled, grain size ASTM 11. AVCO 15 kW HPL C02 laser, focusing telescope F7.

power of the equipment when reasonable speed is a prerequisite for industrial manufacturing,

- Fig 3, CO2, CW, powers 3 to 6 kW. on 4 mm thick,
- Fig 4, CO_2 CW, powers 5 to 6.5 kW on 6.5 mm " ,
- Fig 5, Avco CO_2, powers 6.5 to 12 kW on the 8 mm.

The technique of post welding machining

The nail head and the HAZ dimensions are changing in relation to different experimental parameters and conditions. Since microfissures may occur under the nailhead, in several industrial components which are designed to be welded. the head and the root of the weld bead are machined away; therefore the areas of the bead where the defects **more often take** place, are eliminated. Example of this process is given in Fig. 6, where Inconel 718, 8 mm thick is used for turbine housing, having the normal prewelding heat treatment as follows: 960 "C for 0.5 hours plus 760°C for 0.5 hours. Reliable joints were achieved in age hardened state. The grain size of the base material was ASTM 11 and HV (0.3) 480 in hardness. The aspect ratio in the bead of Fig, 6 is 2.37

and i. 16 mm is the width *in* the middle. Using the above procedure, even microstructures relatively susceptible to microfissuring can be adopted being an advantage, while the disadvantage is the waste of material, the preparation and the post machining of the joint down from 8 to 5 mm.

The distribution of the residual stresses, which is one of the cause of microfissuring. is related to the extension

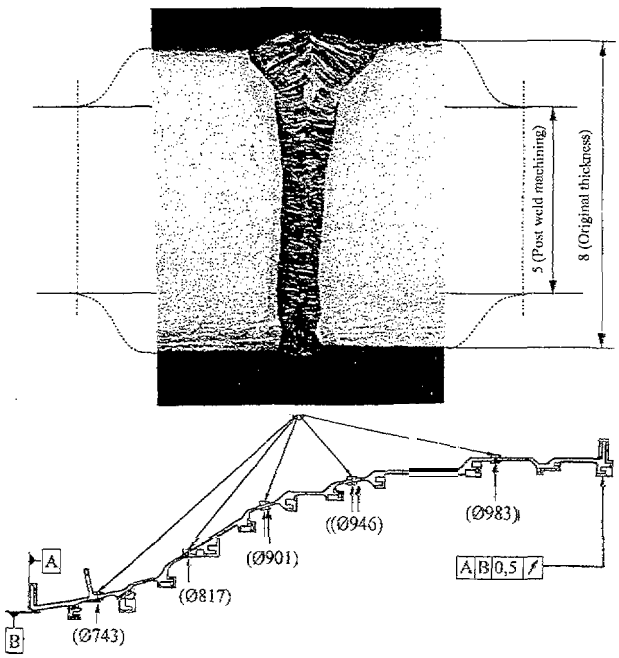

Fig, 6 Cross section of assembled rings and circumferential weld to be made in low pressure turbine housing. The joint tit up is designed for post weld machining of the head and the root of the bead from 8 to 5 mm thick. Top: macro of the weld made by AVCO CO_2 laser at 12 kW and speed of 3.2 m/min.

and the shape of the nail head. The optimisation of the parameters to reduce the nail head extension is favorable to the elimination of the microfissures.

The CO_2 continuous wave and the Nd:YAG pulsed mode lasers produce joints with different nail heads, the other influent parameters being the gas and its pressure at the plasma suppression nozzle and the focal point position. Fig. 2 shows the more uniform and round cross section bead profile achieved by YAG laser which are less prone to microfissuring compared to the ones of Fig. 3 achieved by the CO_2 laser. Since the weldability depends on microstructure and on the thermal history, several researchers [3, 4], investigated the effect of prewelding conditions on micro fissuring. Demonstration was made that fine grain sizes [8] and that a cold work ratio of 30÷40 % could avoid microfissures in sheets 5 to 8 mm thick [9].

Since hot working is, a basic technique used to manufacture aeroengine parts made of superalloys, hot rolled samples were chosen to investigate the possibility of eliminating the microfissures through the prewelding conditions. The materials could be controlled by deformation temperature and work ratios in terms of controlled rolling, enabling the various microstructure to be achieved on the basis of' the dynamic recrystallization theory.

The grain sizes were from 10 to 12 ASTM in commercial materials. The results indicated that the susceptibility to microfissuring of the base materials with residual elongated grain was remarkably reduced, Fig 7 shows the cross section of bead made by high power CO_2 CW laser where the profiles are not regular and have large nailheads. The metallographical examination did not find any micro fissures and static recrystallization was assessed in the HAZ. The elongated grain is about 20-30 % in base materials.

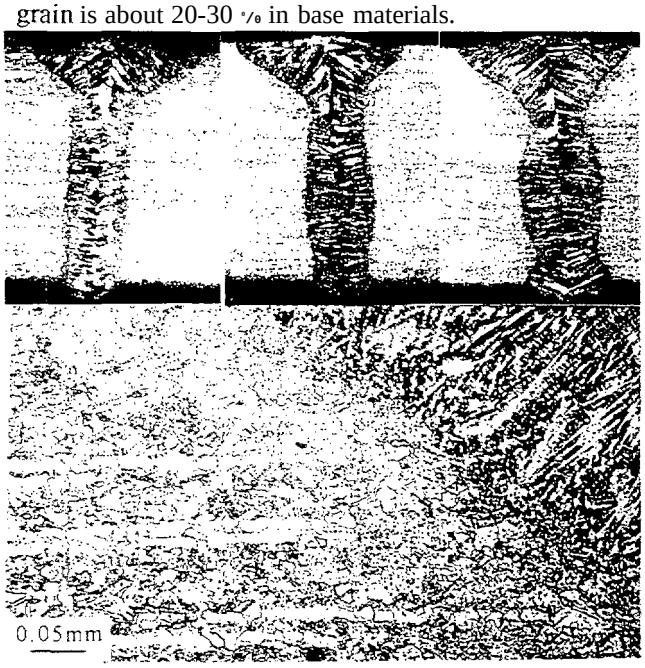

Fig. 7: Inconel 718-4 mm thick with 30-40 % residual elongated grain. hardness HV(0.3) 203. The cross section of bead and of the HAZ show large nail head and the recrystallization. Weld made by CO_2 CW laser (AVCO HPL 15 kW), parameters from left: 3.5 kW-2 m/min, 4 kW-2. 1 m/min, 5.5 kW-2.7 m/min, focus position 0, Helium shielding gas 25 l/rein.

The mechanism of microfissuring.

The most widely accepted is the grain boundary penetration mechanism [10], wherein a migrating grain boundary interacts with liquating matrix particles such as carbides in the HAZ. The liquid enables the boundaries to separate under the welding thermal stress. Since the heat input of laser welding is much lower than conventional arc welding (about one tenth), the real phenomena in the HAZ could be observed distinctly, offering the opportunity to get further information about microfissuring besides simulating methods, The results about microfissures can be summarised as follows:

- They occurs at the end of the melted grain boundary instead of c1osc to the fusion zone (Fig.8).
- They take place in the band of delta phase (Fig 9)
- They occur in the residual elongated grain (Fig. 10)
- They can be eliminated taking the opportunity of the static recrystallization in the HAZ (Fig. 7).

Since those results are difficult to be explained by the penetration model, a segregation mechanism may adapt to these phenomena. There are two reasons which results in depression of the effective solidus of the grain boundary :

a) Due to epitaxial nature of the solidification (<100> in FCC metals) the grain boundary in the HAZ can be linked with the solidification grain boundary in the fusion zone. Segregated Niobium (a key solute of Inconel 718). during solidification is able to diffuse to the HAZ from the fusion zone along this pipeline of grain boundaries.

b) The delta phase Ni3Nb was used to pin down the grain boundary and control the grain size during hot working, this concentrates the Niobium at the grain boundary and, because of the low thermal input during laser welding, the delta phase may only partly solubilize in the HAZ. As a consequence the grain boundary may be melted during welding thermal cycles. and if the local stress is sufficient, the melted grain boundary will separate. Microfissuring takes place in the elongated grain and in the delta band according to these two limit situations. In general the melting of the grain boundary results from the contribution of two metallurgical factors, The tip of the melted boundary suffers from the stress concentration where the initial point of the microfissure is formed.

In cold or hot worked materials with residual elongated grain, static recrystallization will take place in the HAZ if the heat input is high enough during laser welding, thus producing a grain refinement. The mechanism of static recrystallization [1 1] is:

a) Bulging of original grain boundary.

b) Coalescence and growth of subgrains through an increase of perimeter misorientation by additional dislocation and straining respectively,

The new grain boundary migrates away from the delta phase resulting in a clean and greater grain boundary area. During this process the pipeline diffusion of Niobium ceases, The new grains grow, eliminating the deformation substructure and finally the new fine grains are strain free, a fact which relaxes the thermal stress. Thus the microfissuring is restrained by static recrystallization.

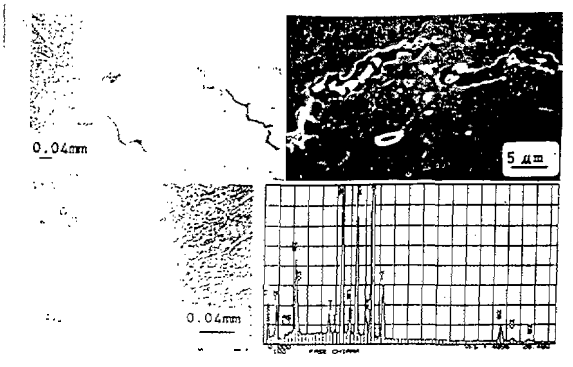

Fig. 8 Microfissuring occur at the end of the melted grain boundary which is enriched with Nb, Ti and Mo.

Fig. 9 Microfissures occur in the delta phase band

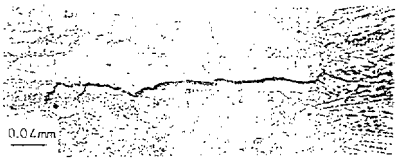

Fig. 10 Microfissures occur in the elongated grains,

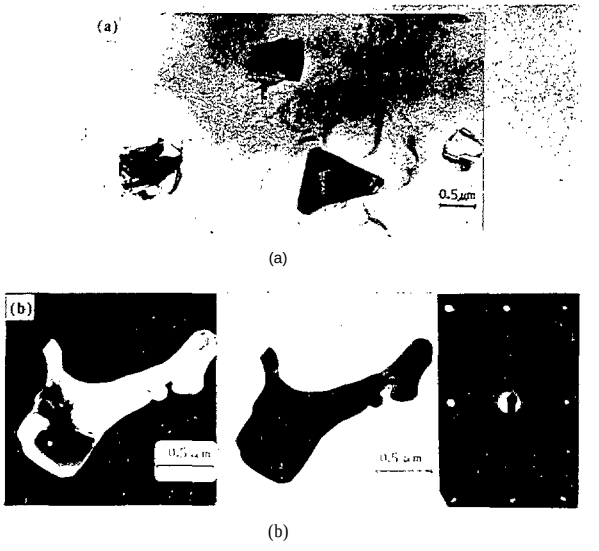

Fig. 11 Isolated carbides in the fusion zone welded by AVCO CO_2 CW laser (left) and the JK706 Nd:YAG pulsed laser (right). The dimension of carbides is 0.5-1 μ m. which were enriched with the Niobium, Titanium. NbC: [112] orientation,

Fig. 12 Suppressed gamma / Laves eutectic in the fusion zone obtained using an AVCO CO_2 cw laser. Laves: [21 12] orientation.

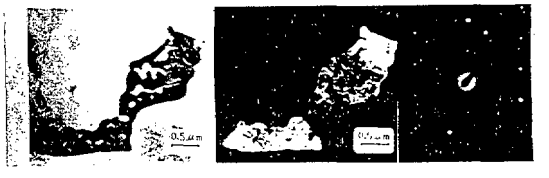

Fig. 13 Fine gamma / Laves eutectic in the fusion zone obtained using a JK 706 Nd:YAG pulsed laser.
Laves : [2 112] orientation.

The microstructure of the fusion zone.

Laser keyhole welding creates a high aspect ratio bead with the rapid cooling speed up to 10000 'K/s [5] The rapid solidification not only increases the undercooking and the nucleation probability that renders very fine structures, (the second harm distance of dendrites is about 2 yin), but also extends the solute volubility that removes heavy segregation and formation of large eutectic. During solidification. the Niobium, Titanium and Molybdenum solutes accumulates at the front of the liquid- solid interface and segregate at the interdendritic

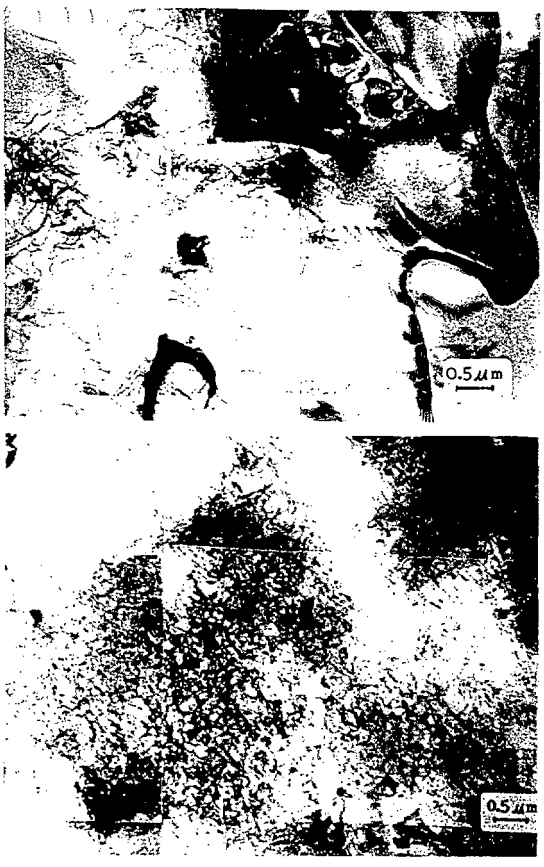

Fig. 14 Dislocations in the melted zone welded by AVCO $C0_2$ cw laser (a) and JK 706 Nd:YAG puked laser (b).

areas where the carbide (NbC, Face Centered Cubic) and Laves Ni3Nb, (Hexagonal $MgZn_2$-type) form. The eutectic of Gamma/NbC was suppressed in the fusion zone welded by both CO_2 CW and by Nd:YAG pulsed lasers, The 0.5-1 μm carbide was also present inside the dendrites (Gamma), Fig. 11. This results from the extension of the nucleation probability due to rapid solidification and since the crystal type of carbide and the Gamma is the same (FCC), the heterogeneous nucleation of Gamma was available. The eutectic of Gamma/ Laves was suppressed in the fusion zone welded by CO_2 CW laser, Fig. 12, in the one welded by Nd:YAG pulsed laser, Fig. 13, the eutectic had a dimension of 0.5-1 micron. Since the heat input of the Nd:YAG pulsed laser is higher than the $C0_2$ CW one, during welding and there is a gradient of solidification rate from the boundary to the centre in the weld pool, these results are reasonable, There is a higher density of dislocation in the fusion zone welded by $C0_2$ CW than in that welded by Nd:YAG pulsed laser (Fig. 14).
Dislocation was introduced during rapid solidification and propagated by thermal stress. Both the cooling speed and the residual stress have a higher value in the samples welded by CO_2 CW laser [12].

Post welding heat treatment
The aim of post welding solution heat treatment is to solubilize the Nb-rich Laves and produce a homogenized fusion zone. The temperature of the solution depends on the degree of segregation produced by laser welding which is lower than arc welding and similar to the Electron Beam. If the temperature is too high. the grain of the HAZ will grow first. followed by the base material: thus fatigue properties will be degraded. The need is the development of the maximum mechanical properties of the fusion zone. the HAZ and the base at the same time. moreover the optimum procedure of post welding heat treatment must consider the balance among three regions in which microstructures arc so different. The lowest temperature must be determined at which the Laves phase begins to disappear, the fusion zone can be homogenized and the tendency of grain growth in the HAZ and in the base material can be minimised.
For most applications. Inconel 718 receives onc of the following two heat treatments:
(1) 927 'C - 1010°C solution and ageing.
(2)1038 °C -1066 'C solution and ageing.
The low temperature solution develops the tine grain which produces the highest fatigue strength. The Laves solution initial temperature is about 1010 °C (Fig. 15). Many Delta phases precipitate at the interdendrites region at the 960 °C solution heat treatment (Fig. 15). These indicate that the temperature of the post welding solution heat treatment should be higher than 1000°C. The high temperature (1038°C - 1066°C) solution is preferred in tensile limited applications because it produces the best transverse ductility in heavy sections, impact strength and low "temperature notch tensile strength. At these temperatures the laves phase of the fusion zone dissolved completely and only NbC was present. The angle of trigonal grain boundary yielded to 120010 each other. The heating speeds have to be low enough, or else the two stage heating procedure should be used to prevent grain growth in the HAZ.

Fatigue tests.
As a consequence of the evolution of the microstructure with the post weld heat treatment the fatigue tests were devised in the following conditions:
Preweld treatment: as received, Grain size ASTM 11.
Post weld treatment A), traditional in SNECMA:
-760 °C x 5 hr + cooling at rate of 50 'C ± 20 °C/hr to 650 "C x 1 hr + air cooling. defined as "direct ageing".
Post weld treatment B). devised as a consequence of the metallurgical tests by RTM:
-1010 "C x 1 hr + the above direct ageing.
Both treatments was adopted for CO_2 and Nd:YAG laser welding. Fatigue test were performed on as welded and after machining away the head and the root of the bead, the test temperature was 650°C.
Fig. 16 shows the results on CO_2 laser weld, with Snecma treatment A) and with+ without machining;
Fig, 17 shows the results on Nd:YAG laser weld. with RTM treatment B) and with + without machining.

3. APPLICATION OF THE 13.4 SIC RESEARCH TO TYPICAL AEROENGINE COMPONENTS MADE OUT OF SUPERALLOYS.

Exhaust frame for CFM 56 engine
In the high-temperature section of the aeroengine, the exhaust frame, which is a static structural component, is made up of the following Inconel 718 items, as shown in Fig. 18. Starting from the central ring they are:

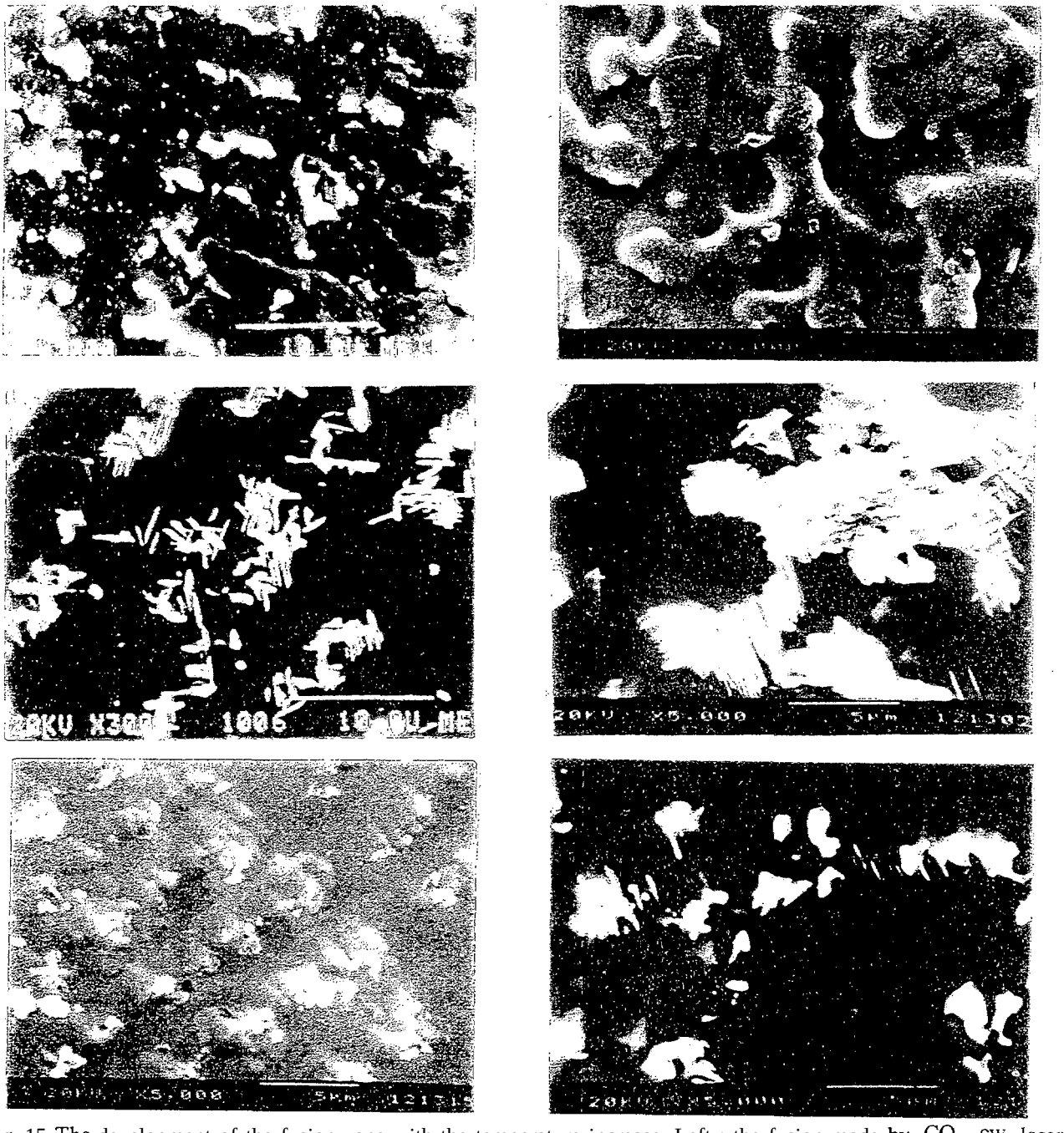

Fig, 15 The development of the fusion zone with the temperature increase, Left : the fusion made by CO_2 cw laser, Rigth: the one by Nd:YAG pulsed laser, From top: A, B, as welded; C,D, 960 'C x 1 hr; E,F, 1000 °C x 1hr.

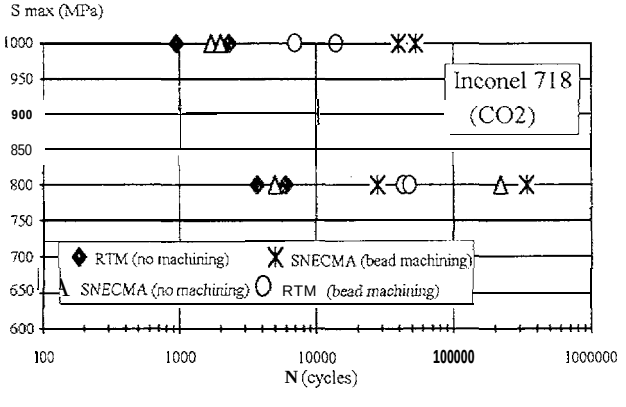

Fig. 16 Results from fatigue tests at 650 °C on Inconel 718 specimens welded by CO_2 cw laser.

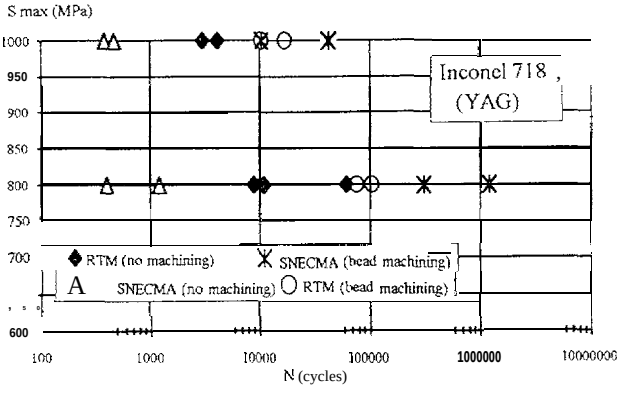

Fig. 17 Results from fatigue tests at 650 "Con Inconel 718 specimens welded by Lumonics JK 706 Nd:YAG.

-housing for bearing support having 12 short radial arms (cast Inconel 718, thickness 2 to 4 mm)
-12 radial wing-profile arms (rolled Inconel 718) welded to the above
-12 plaques (cast Inconel 718, thickness 2 to 4 mm), each having a short radial harm
- 12 spacing plaques without arms made of cast Inconel 718, thickness 2 to 4 mm. (All the above plaques are welded together to form the outer virole ring).

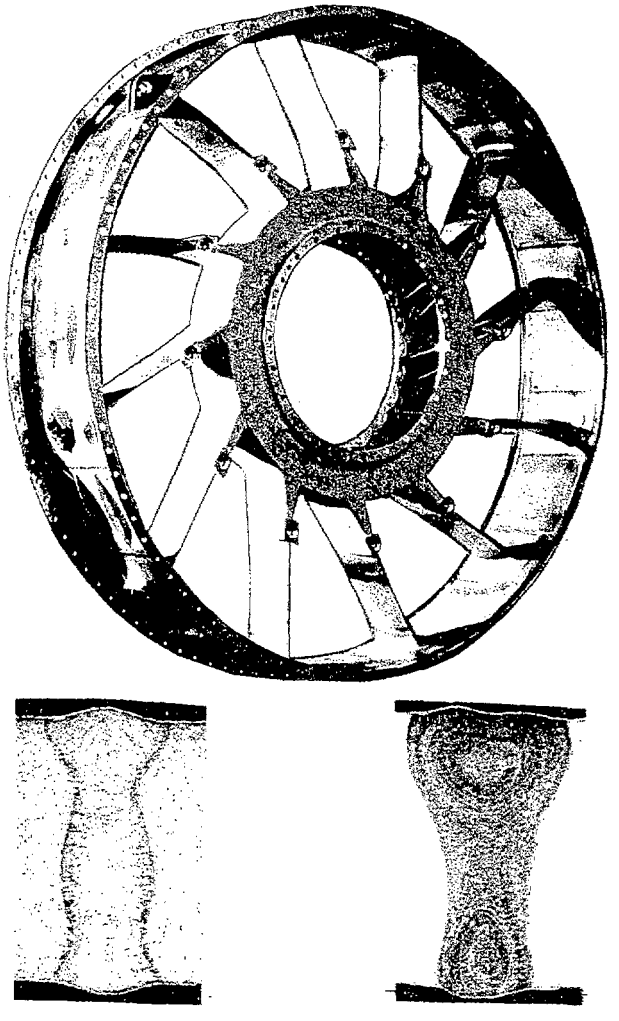

Fig, 18 Exhaust frame (dia. 1000 mm) made of Inconel 718 cast, rolled and forged items
Bottom:" Macrograph of beads obtained using CO_2 CW (left) and YAG pulsed (right) lasers.

-2 flanges made of forged Inconel 718, thickness 2 and 4 mm, welded onto the faces of the outer virole ring.

The primary purpose of the research was to use lasers to weld the above items, which are currently joined using TIG, EB and plasma welding. The second aim was the design of the component, which was to be made up of sheet metal items, so as to reduce the weight compared to the cast structure.

CO_2 laser welding was chosen for manufacturing the prototype owing to the availability of this source at the premises of the partner responsible for prototyping this component. In this research, laser cutting and rewelding experiments were also made: after the 24 sectors had been longitudinally joined to form the virole, circular cuttings were made to obtain flatness of the outer virole ring faces. Then the two flanges were welded to the faces.

Low-pressure turbine casing

This mock-up of an acroengine part is made of Waspaloy (thickness 2 mm; diameter 400 mm; length 500 mm). Purpose of the research was laser cutting and rewelding in order to simulate both manufacturing of new parts and overhauling of used ones. The following manufacturing operations were adopted:

-rolling of two half-cylinders and mechanical machining of their generating edges to be adapted for butt welding
-chemical etching and setting in the jig
-spot tacking and autogenous butt welding along the longitudinal edges to obtain a cylinder
-laser cutting of 3 rings (Fig. 19, top)
-facing of the two edges of t he first cut using a lathe
-autogenous butt welding of two of the above rings
-autogenous butt welding of the third ring. For organisational reasons. it was not possible to use the same laser for cutting and welding. The CO_2 laser was used for cutting. while the JK 706 1 kW pulsed YAG laser was used for welding. If the small thickness of the part is considered. no post-weld machining aimed at eliminating undercuts at the top and root of the bead is possible: hence. undercut-free welds are required. By adopting suitable pulse shape. frequency, energy and speed. a weld pool dynamics was obtainable that resulted in undercut-free joints, as shown in the cross section of Fig. 19. In this application. it is more difficult to obtain the same undercut-free joints when the $C0_2$ CW laser process is used. owing to the higher welding speed needed to achieve the same cooling rate. The cutting parameters were as follows: power 6(N W; frequency 1000 Hz; speed 0.1 m/min; helium gas pressure 14 bar; focal length 2.5". The welding parameters were: power 760 W; frequency 33 Hz; speed 160 mm/min; pulse width 7 ms. Analysis revealed that the same weld quality was achieved on both the machined and the as-laser cut rings. However. while refinement is needed to eliminate some residual porosities, the process proved attractive because, when adequate tooling is used on the same laser station, the elimination of sheet metal losses from the rolled items can produce semifinished parts ready for welding, thus avoiding mechanical machining.

Compressor deswirl

This part belongs to the compressor of a helicopter engine. It is made of rolled sheets of Inconel 718. The outer ring has a diameter of 340 mm, a width of 40 mm and a thickness of 1 mm; the inner ring measures 320 mm in diameter and has a width of 25 mm and a thickness of 1 mm. The latter is conical so as to produce a divergent-flow section (Fig. 2(I bottom right). There are 72 slots, 0.73 mm wide and 23 mm long, made in the rings, each shaped like the sector of a circle, In the current manufacturing process, the slots are cut by electron discharge machining and accommodate 72 curved vanes made of 0.7-mm thick Inconel 718 sheet. Currently TIG with filler metal is used both for joining the outer ring and for welding the vanes to the outer and inner rings. Brazing is also adopted for the above process. whilst EB welding is at an advanced stage of

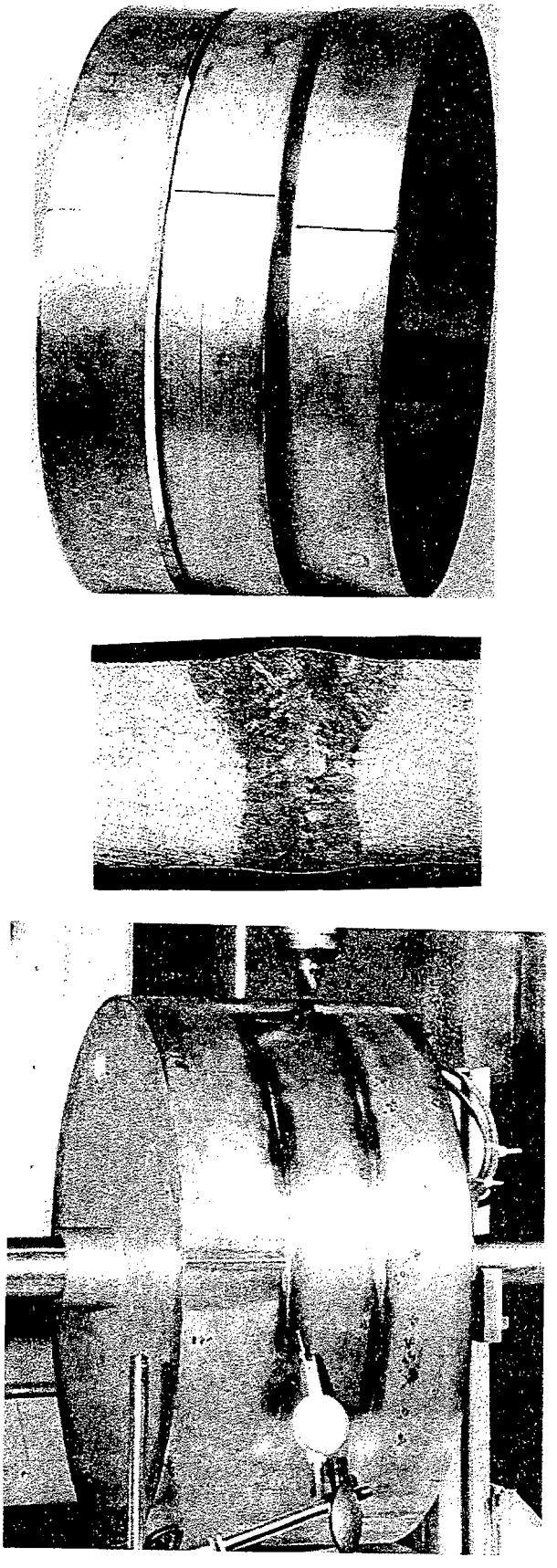

Fig. 19 Low-pressure turbine casing made of 2-mm thick Waspaloy sheet. Top: After longitudinal weld and laser cutting of the 3 rings. Centre: Typical weld bead. Bottom: Rewelding by YAG laser.

development at the Customer's laboratory. After evaluation of the advantages and disadvantages of conventional welding techniques, the manufacturer also decided to try out laser technology, encouraged by the advantages of using the same laser station for:

-cutting and welding the outer ring
-cutting the slots in the inner and outer rings
-welding the vanes to the inner and outer rings,

and by such advantages as:

- low distortion. duc to low thermal input. which avoids the post-weld adjustments at present needed when high thermal-input welding techniques are used
- the economic benefits that the manufacturer expects will result from the new manufacturing cycle and organisational streamlining.

The experimental results so far achieved on this component are shown in Fig.20. The 72 slots were cut by a YAG laser using high-pressure argon.

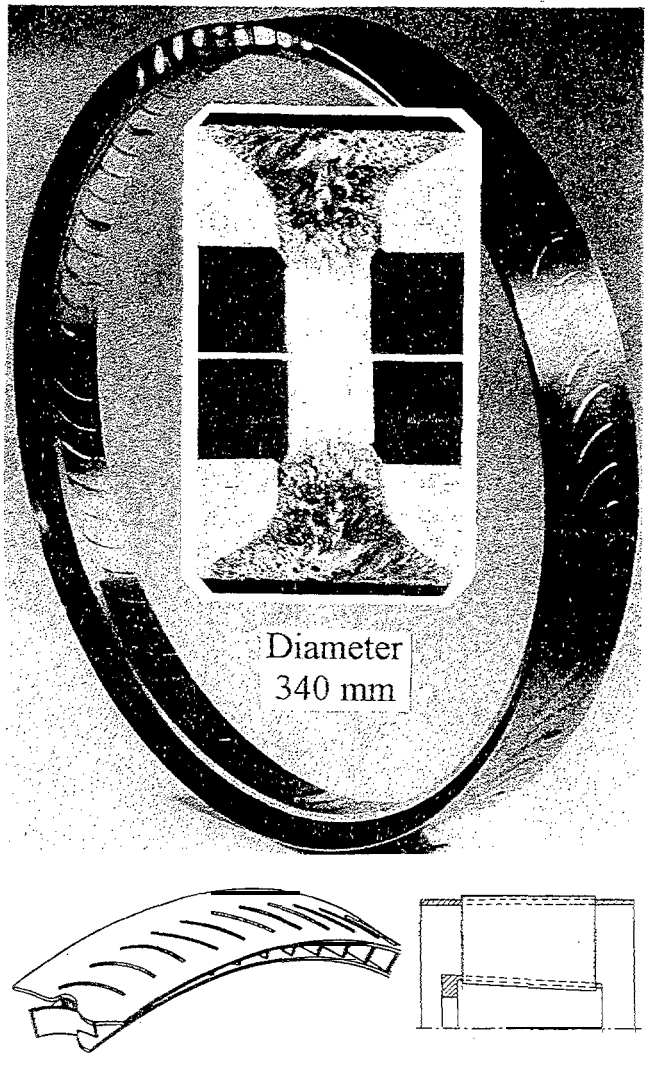

Fig. 20 Compressor deswirl made of Inconel 7 18, thickness 0.7 mm.

Geometrical accuracy of 0.03 mm was achieved on the width of the laser-cut slot. When inserted into the slots, the vanes protruded 0.3 mm from the outer surface of the rings: thus the need for filler metal was eliminated. The Lumonics Multiwave 2000 YAG laser was used. The most significant weld beads were achieved with the following parameters: pulse frequency 100 Hz;

continuous power 950 W; peak power 1950 W; speed 0.75 m/min; fibre optics and focusing length 110 mm; helium shielding gas. Fig.20 shows the sections of one vane welded to the rings. In line with Customer specifications, a bead penetration from 0.6 to 1 mm was achieved. After welding, the diametral shrinkage. flatness and dimensions of the divergent-flow duct were acceptable, At the present stage of the research. two components have so far been made which satisfy some of the specifications. Improvements in the welding system are planned. and so the other specifications are expected to be met.

Containment ring

This component forms part of a helicopter engine. Fig. 21 (top) shows the longitudinal section with the items to be joined, along with the material used. L 1. L2. L3, L4 arc the welds to be made. At present EB or TIG are used, and the items are assembled in the proper aligned position thanks to the stepped edges on the ring and on the flange. The front and rear shells are obtained from roiled sheet, and after being rolled into a cylindrical shape, are closed by a longitudinal TIG weld. In agreement with the manufacturer. the following alternative solutions were adopted: elimination of the stepped edges using a suitable expandable jig for correct alignment of the rings. and circumferential welding using the high-power Lumonics Multiwave 2-kW YAG laser. Before carrying out circumferential welding, the shells were spot tack-welded along all the joints after all the items had been packed on the jig
chuck, The welds obtained with a 980-W CW laser at a speed of 0.85 m/min are shown in Fig. 21. The welds were porosity-free, and hence acceptable, The total of four welding cycles caused a longitudinal shrinkage of 0.5 mm. Diametral shrinkage of L 1, L2. L3 "was negligible whilst L4 shrinkage was 0.2 mm.

Support shroud for helicopter engine

Fig, 22 (top) shows the section" of the part, which is made out of four items: No.1 is the basic support. ring (Inconel 718); Nos. 2 and 3 arc 0.7-mm thick strips made of oncology 909; No. 4 is the flange made of Inconel 718. The strips are first wound over the annular grooves, and then welded in position, thus creating the annular interstices for cooling the component. At present the annular welds are made by EB, and the gaps between the end edges of the strips are closed by TIG longitudinal runs on a separate station, The purpose of the research was to evaluate the feasibility of reducing manufacturing costs, at the same time meeting the quality specifications set by the Customer. The Lumonics 706 1 kW pulsed YAG laser equipped with fibre optics was used. The welding sequence is indicated in the figure by the letters a), b), c), d), e). Weld d) was performed using a 60° beam incidence, before the final weld (e) of the flange was made. After deoxidisation and degreasing, the strips were wound and clamped by a ring around the basic support. An essential feature of ibis phase was the accurate overlapping contact between the strip and its substrate, as well as the correct gap between the end edges of the strip. The following joining cycle was adopted: spot tacking, continuous tacking, deep welding. Total penetration was 1.3 mm for a), b), c), and d), while for e) the in-depth penetration was 3.5 mm.

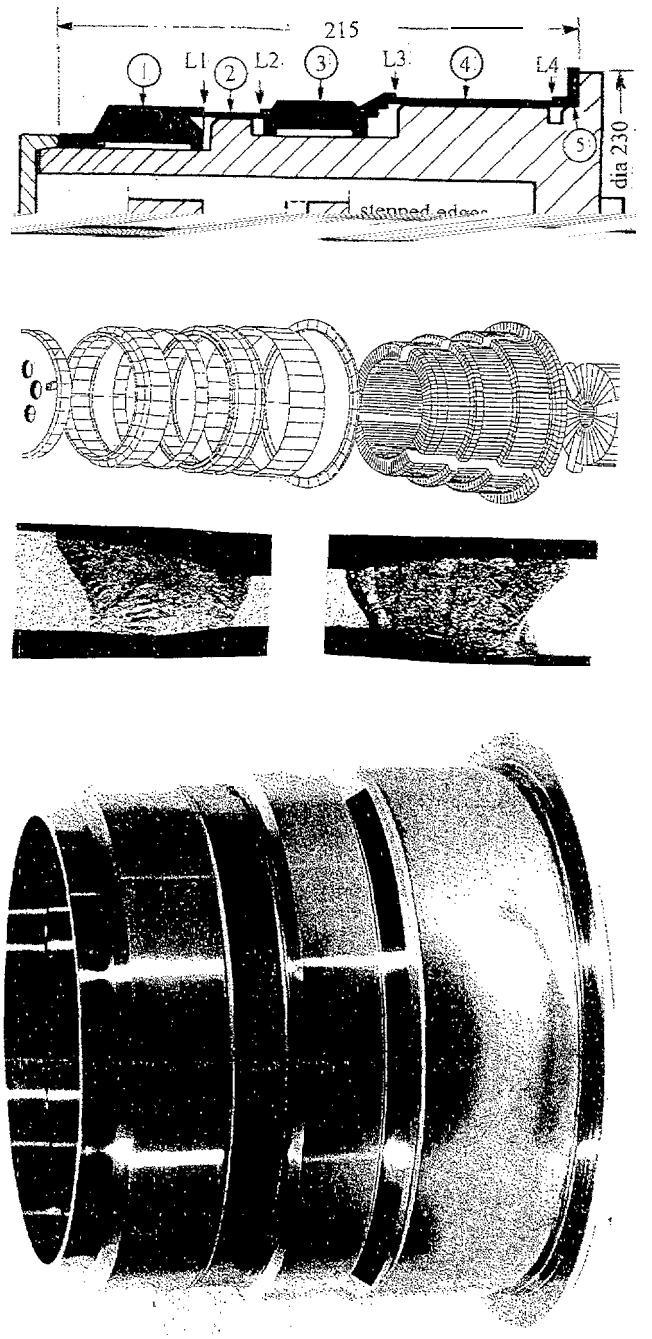

Fig.21 Containment ring. From top down: Longitudinal section: assembly on jig: weld bead; assembled part. Legend: 1) front ring. 1.4 mm In 625; 2) front shell, 0.8 mm In 718; .3) rear ring, 1.4 mm In 625; 4) rear shell, 0.8 mm In 718, 5) flange, 1.4 mm In 718.

The final result is shown in Fig. 22 (bottom). Among the peculiarities of this process, worthy of notice is the fact that the end edges of the strips can also be welded on the same station. This represents one of the major economic advantages.

Welding of cover plates on turbine blades/ vanes

Typical superalloy used in the manufacturing of these parts arc: B 1900, MAR-M-247, RENE 80, Single Crystal 2000, They are obtained by casting, and they are classified as partly unweldable because very susceptible to cracking. The adequate closing of the cavity at the blade root, which is consequent to casting, is currently made by brazing, It is economically and technically a

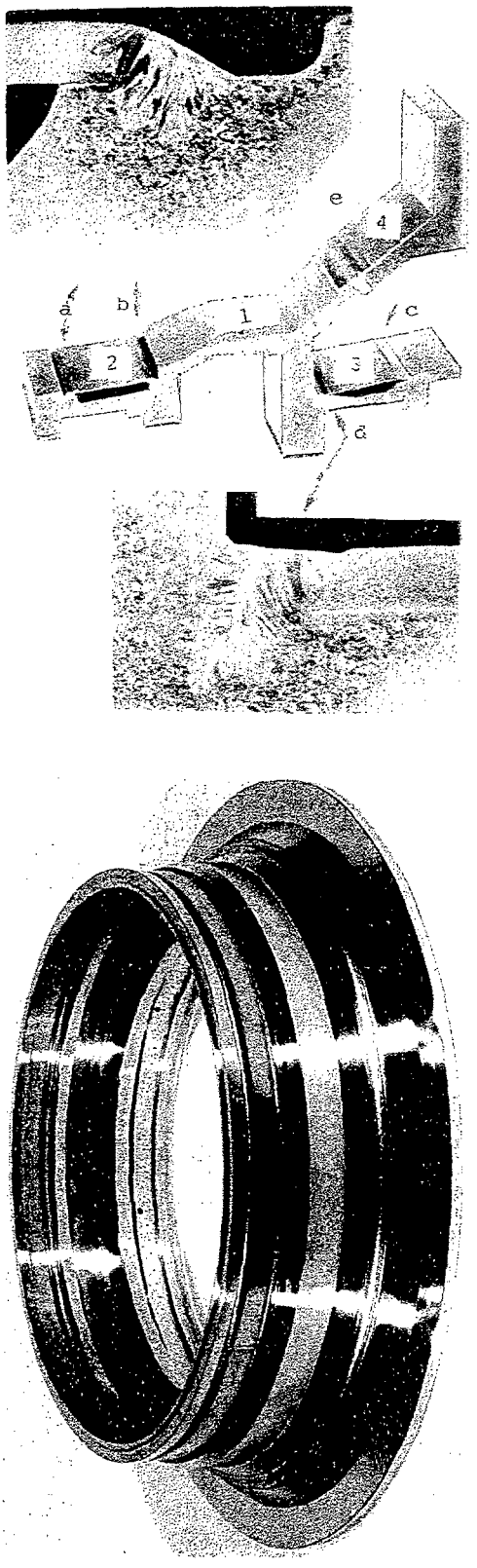

Fig. 22 Support shroud (Inconel 718: diam. 320 mm) Top: Section of shroud with macrographs of weld bead sections. (1) basic support;(2 & 3) welded strips (Note interstices for cooling); (4) welded flange. Bottom: Finished assembly welded by Nd:YAG laser.

very relevant step of the manufacturing. due to the large amount of manufactured turbine blades and vanes. both for the market of new engines and for the overhauling. If welding is chosen for the purpose and when the metallurgical and structural aspects arc considered. the most suitable solution to the problem is by the application of cover plates made out of Hastelloy X (Fig. 23). Moreover the adequate application of the thermal input to the overlapping parts to be welded. will allow to generate the balanced dilution of the critical metallic elements (Al and Ti) into the melt pool and will result in minimising or in the absence of microfissuring. Fig. 23 represents the experimental conditions adopted: on the left. by the beam focused on the surface, a deep penetration can be achieved. while on the right. by defocusing, the conduction welding can be obtained. To the above conditions the following ones were added: focus position referred to the edge of the plate (XF). the CW and pulsed mode by CO_2 and by Nd YAG using adequate pulse shape. The research was developed jointly by MTU and Lumonics.

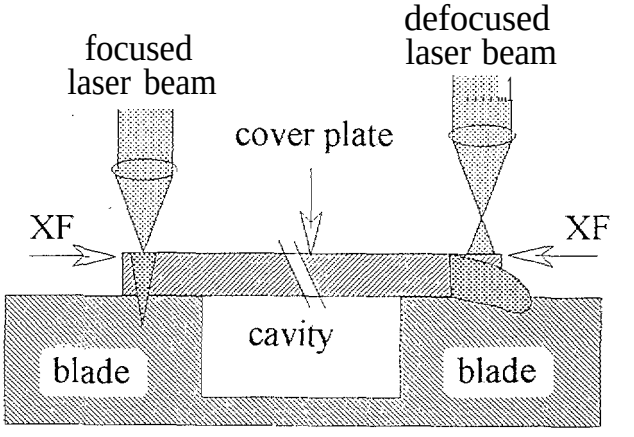

Fig. 23 Scheme of deep penetration (left) and of conduction welding (right) of cover plates on blades.

Among the significative results the onc given in the Fig. 24 represents Hastelloy X cover plate welded to the Nickel cast alloy Single Crystal 2000, using the CO_2 laser. On the top the deep penetration is shown which was made using the following conditions:
Power 1 kW, pulsed mode, pulse ratio 2/5, speed 0.6 m/min, focal length 5“, focus position O mm, nozzle to piece distance 6 mm, nozzle diameter 5 mm, Helium flow shielding gas.
The bottom Fig. 24 represents the heat conduction weld of the same metals using the following conditions:
Power 1.3 kW, mode CW, welding speed 0.35 m/min, focal length 5“, focus position 6 mm, nozzle to work piece distance 12 mm. nozzle diameter 5 mm, Helium gas. Some microfissures were assessed mainly in the deep penetration welding (macro top picture) which is more prone to microfissuring than the conduction one where absence of defects was assessed, However the joints are conform to the company specifications also considering that this joint is much stronger than the conventional brazing currently used.

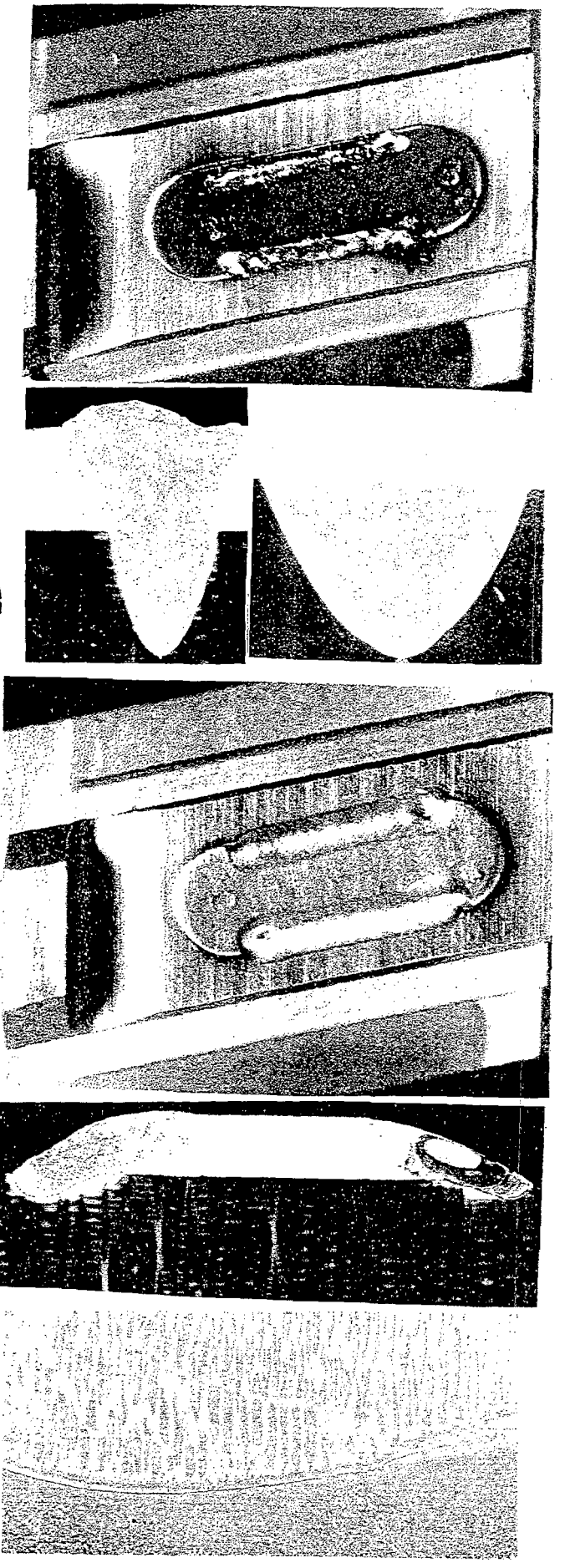

Fig. 24 Welding of Hastelloy X cover plates on Single Crystal 2000 blades. Top: deep penetration, bottom: conduction welding.

4. A PPLICA TION OF THE BASIC RESEARCH TO TYPICA L COMPONENTS MA DE OUT OF TITA NIUM ALLOYS.

Bearing support for aeroengine

One of the partners in the project has just entered the market with a new very high-thrust turbofan. Innovations in both design and manufacturing technology have been introduced. As regards laser technology, the welding of some components, even of large dimensions. is already a reality, whilst for other components. e.g.. bearing supports for aeroengines (see Fig. 25). the process is still being optimised. The aim of the research was to build a cone-shaped bearing support from 1 3-mm thick Ti6Al4V sheet. the cone being joined along the generatrix using a laser. The basic welding tests were conducted on flat specimens using butt joints without filler metal, After welding, the sheet making Up the cone was machined in depth to create lightened, and at the same time reinforced, structure. The weld. which

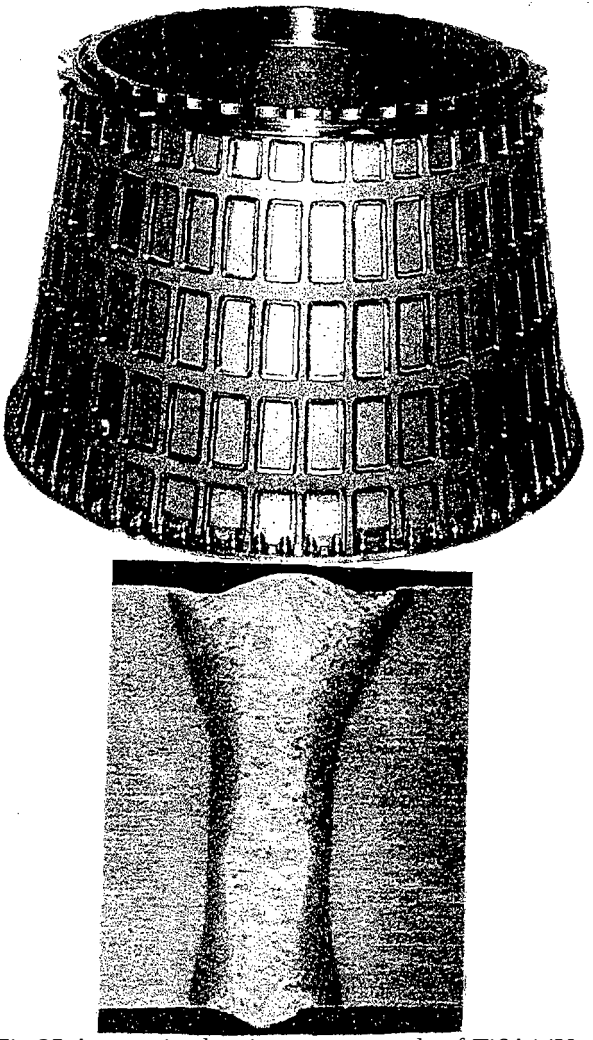

Fig 25 Aeroengine bearing support made of Ti6A14V. Thickness 13 mm; diameter 820 mm; overall length 450 mm; weight 60 kg.
Bead section: AVCO CO_2 laser: power 12 k W; speed 1.5 m/min.

remains part of the Longitudinal ribbing, will be machined on the top and at the root, so that the typical defects occurring in those parts of the weld will be eliminated, An AVCO Everett 15-kW CO_2 laser source was used. The most significant result is represented by

the cross section shown in Fig.25, which was obtained using an F7 telescope, the focal length of which is equivalent to 950 mm. The parameters were as follows: power 12 kW; speed 1.5 m/min; focus position +6 mm above specimen surface. Helium was used as shielding gas on both sides, and a new nozzle was developed [or this high-power application. The shielding action resulted in a very shiny appearance of the weld. and at X-rays on average 2 pores of 0.2 mm in diameter each were found over a length of 450 mm. This result met the quality specifications set by the manufacturer.

Repairing of titanium blades by the combination of cutting and rewelding by laser.

The refurbishment of large dimension single blades and of the ones integrated in monolithic multibladed rotors, is economically very relevant both for the industry operating at the maintenance of parts damaged or worn-off due to operation as well as in the elimination of defects which cause rejections occurring during the manufacturing of very expensive complex static or rotary structures. The repair cycle has the following main phases: cutting away by laser the damaged sections within the standard limits, subsequent welding by laser of an adequate patch to the remaining blade in order to regenerate sufficient volume of metal for the subsequent phase of milling and grinding used to obtain the correct functional profile according to the original design. At MTU the cutting and welding were performed on the same laser station by adequate fixtures and laser heads, thus demonstrating one of the advantages of the procedure.

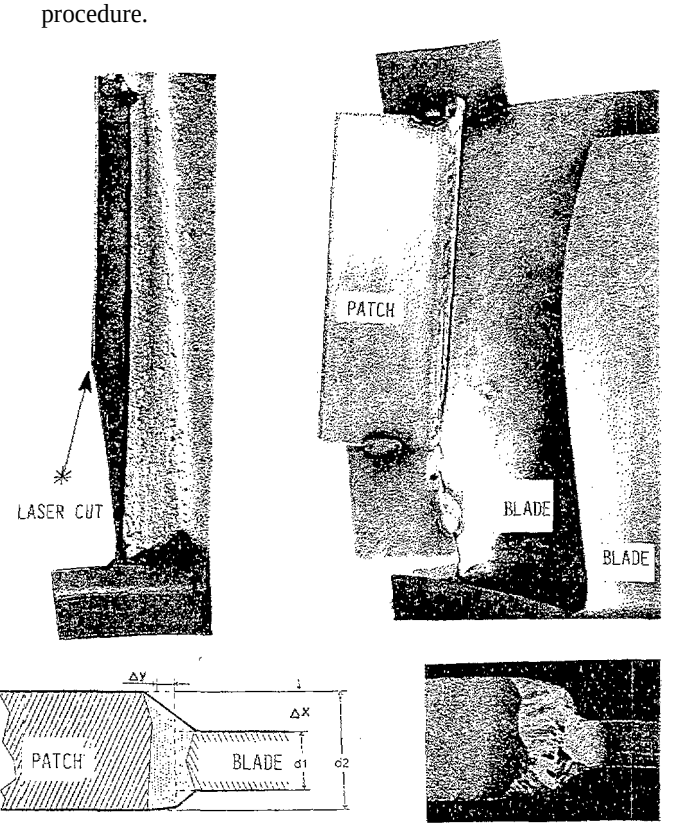

Fig. 26 Titanium 6242: repair of aeroengine compressor blades. Top left: the damaged leading edge was cut by CO_2 laser, right: using the same laser station a patch was welded on the cut edge. Above from left: geometry and section of the joint patch to blade.

In Fig.26 the result is given of the damaged leading edge of one blade made out of Ti 6Al 2Sn 4Zr 2M0. the thickness is varying from 0 to 2.5 mm. in the detail is the cut section, The cut roughness of Ra 2 μm and geometry were acceptable. dross and oxidation were absent and the remelted layer was not influent on the subsequent autogenous butt weld. therefore the surface was ready for the welding of the 4 mm thick patch without intermediate machining. The parameters and conditions were as follows: CO_2 laser Wegmann Baasel 2.5 kW used at 700W CW Cutting speed 2m/min. gas Argon at 18 bar: welding power 2.2 kW. speed 1m/min using Helium as shielding. The Fig. 26 shows a patch welded to the blade and the detail shows two significative sections of the joint demonstrating absence of underfill and since X-rays inspection revealed absence of porosities, the part is suitable for the subsequent machining phase.

The same procedure was tested on the blades of the integral rotor made out of Titanium IMI834.

Low-pressure turbine housing

This part of the aeroengine is made up of several conical rings welded together to obtain the structure shown in Fig. 27 (centre). Ti6Al4V (thickness 8 mm) was used. The project included the demonstration of a refurbishment procedure using laser technology. The current cycle is as follows:

- Cutting by plasma or laser in the position indicated by "laser beam" in Fig. 27 (bottom) to separate the rings
- Refurbishment of damaged internal parts
- TIG cladding on the cut faces using Ti6Al4V filler wire by adding more material than that lost from cutting
- Facing of cladding to an adequate dimension to restore the original axial length of the ring, plus the amount for the subsequent welding shrinkage to be compensated for
- EB welding.

The following alternative cycle was decided on:

- Cutting of the ring using a CO_2 laser and high-pressure inert gas to avoid oxidation of the cut faces
- Refurbishment of internal parts
- Laser cutting of the Ti6Al4V filler metal spacing strips shaped as arcs of a circle, 0.65 mm thick and 10.5 mm high
- insertion of the strips between the two rings and packing into the jig
- Tacking and deep welding using CO_2 laser.

The macrograph (Fig. 27, bottom) shows the cross section of the weld bead adopted. This was obtained using a Rofin Sinar RS 6000 CO_2 laser: power 6.7 kW; speed 0.6 m/min; focusing mirror 150 mm focal length. One of the rings having a diameter of 800 mm is shown in the figure (top). The above cycle cuts down considerably on manufacturing time.

Titanium 6 Al 4 V engine frame for aircraft.

This typical tubular lightweight structure. shown in Fig. 28, holds the turbopropeller under the wings of a typical regional transport aircraft, In this structure the diameters of the tubes are changing from 40 to 60 mm and the thickness from 1 to 4 mm. according to the increasing power of the engine. In current manufacturing the orbital GTAW is used due to the restricted access at the nodes areas where the

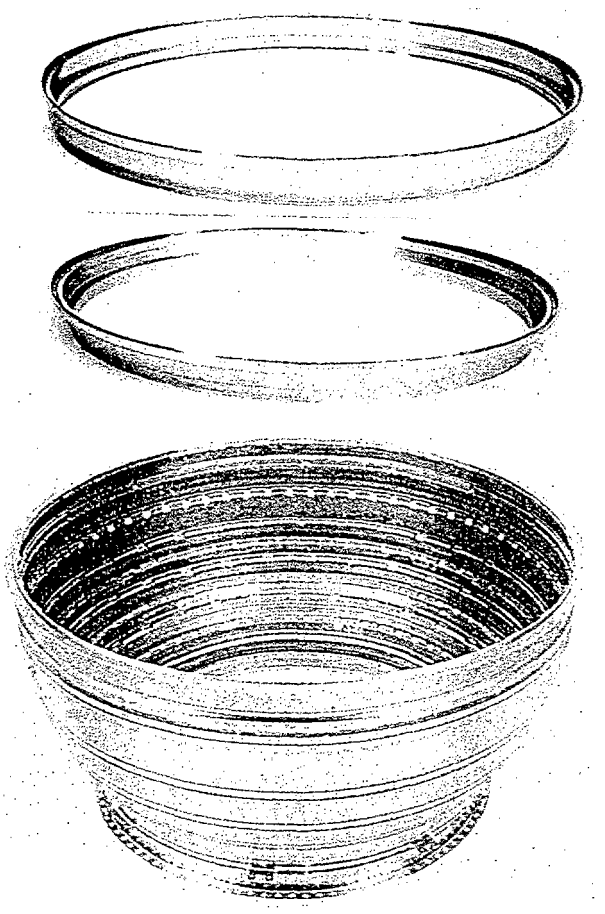

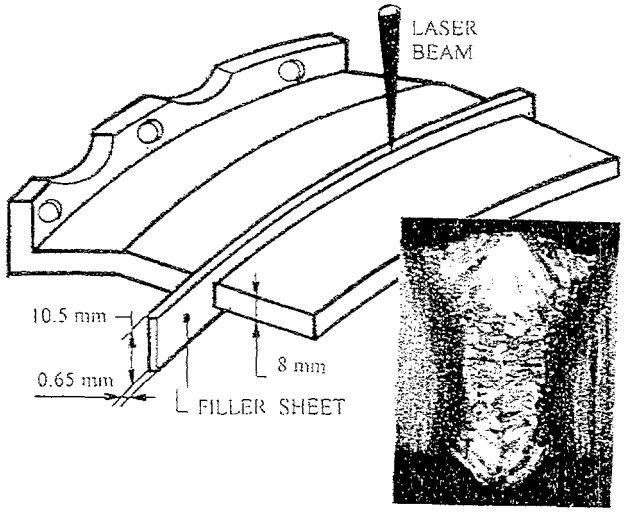

Fig. 27. Low-pressure turbine housing made of Ti6Al4V. Cutting and rewelding using a CO_2 laser for parts maintenance.

Fig. 28 Engine frame for aircraft: Ti6Al4V. From top: -the assembled tubular structure, -the pipes converging into the nodes, -segment of pipe with conventional bead made by GTAW (left) and by Nd:YAG laser (right), - fitting configuration for laser weld and result of the joint without 'filler metal, -fitting for conventional GTAW welding method.

circumferential welds are located. Total of 30 joints are needed for the assembling, therefore high heat input results in final deformation of the structure in particular

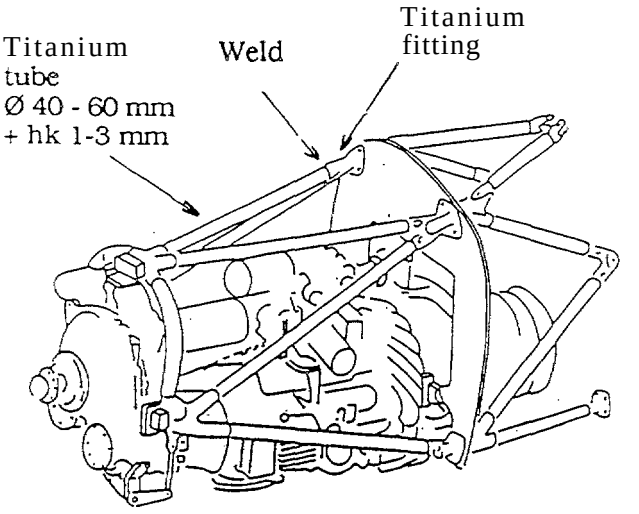

Engine mount with the engine

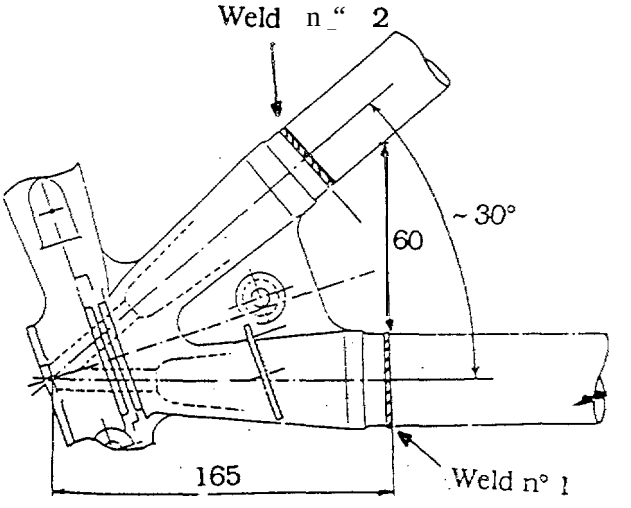

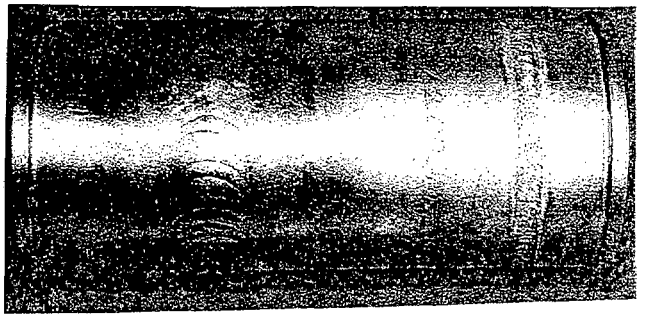

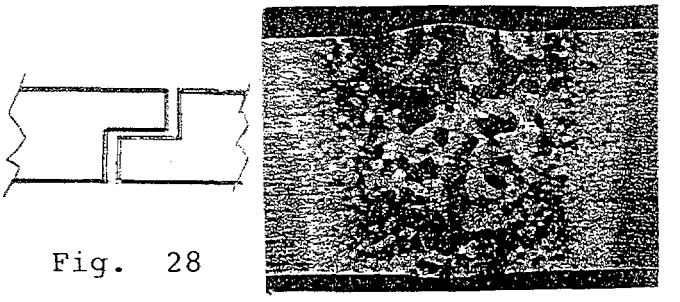

Fig. 28

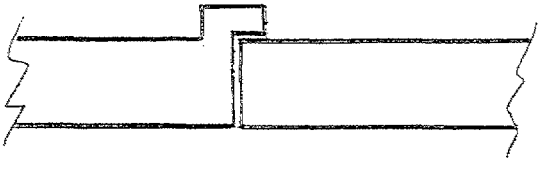

when pipe thickness is over 2.5 mm. Therefore laser technology is favorably regarded in order to reduce thermal inputs even for the joints where the 4 mm or higher thickness pipes arc used according to the planned future aircrafts. The basic welding tests were performed using both CO_2 and 1 kW Nd:YAG with optical fibre. This one is considered to be the most suitable because the optical fibre can conveniently carry the beam in this complex structure. In Fig. 28 the basic weld joint using the Quantel 1 kW Nd:YAG laser on the 2.5 mm thick pipe is shown. The following parameters were used: average power 600 W, repetition rate 30 Hz. Speed 125 mm/min. Helium shielding gas, The detail macro of the section demonstrates the correct blending of the weld bead with the surface of the base metal. In the picture. the comparison is made with the conventional GTAW (the joint on the left), demonstrating the larger section of the joint, which induce increased deformations of the final structure.

Spherical reservoir for space applications

The aim was the manufacture of lightweight spherical reservoirs in 2-mm thick Ti6Al4V. Two half-shells were to be welded together along their equator, the joint being sputtering-free inside the reservoir and smooth on the outside. To withstand the very high pressure of the fluid inside and at the same time obtain a light-weight structure, filament winding is planned to achieve a final thickness of sufficient strength. The partner, Aerospatiale, built the half-shells from 12-mm thick sheet, using the superplastic forming process. A half-shell is seen in Fig. 29 (top). The subsequent operations for manufacturing the reservoirs were carried out at RTM, as follows: cutting of the loss flange and of the polar holes using a CO_2 laser pulsed at 1000 Hz, average power 1200 W. speed 165 mm/min, helium gas pressure 15 bar. and nozzle diameter 1 mm (Fig. 29 top). The next stage was machining of the 4-mm thick stepped chamfer. as shown in the diagram (centre), and machining down of the structure adjacent to the chamfer to 2 mm to simulate the actual final thickness of the shells. The non-through weld joint penetration of 3 mm was chosen to avoid sputtering on the internal surface and to allow for compensation of any strength decrease due to possible defects. The cross section of the weld is shown in the macrograph. Welding was performed at RTM using a Rofin Sinar RS 6000 CO_2 laser. The welding parameters were: power 4 kW, speed 3.7 m/min, focal length 150 mm, focus position +3 mm. The cosmetic run parameters were: power 4 kW. speed 1.4 m/min, focus position +23 mm. The final result is seen in Fig.29 (bottom).

5 FA TIGUE TESTS ON TITA NIUM 6Al 4 V SPECIMENS

Titanium alloy specimens were Low Cycle Fatigue tested at room temperature, as shown in the diagram of Fig. 30. The results are correlated to the typical weld bead geometry, which represents the optimisation that could be achieved by the different partners seeking to meet the specifications on undercut values for static parts. However, the results cannot be taken as an index of the quality of the commercially available equipment used.

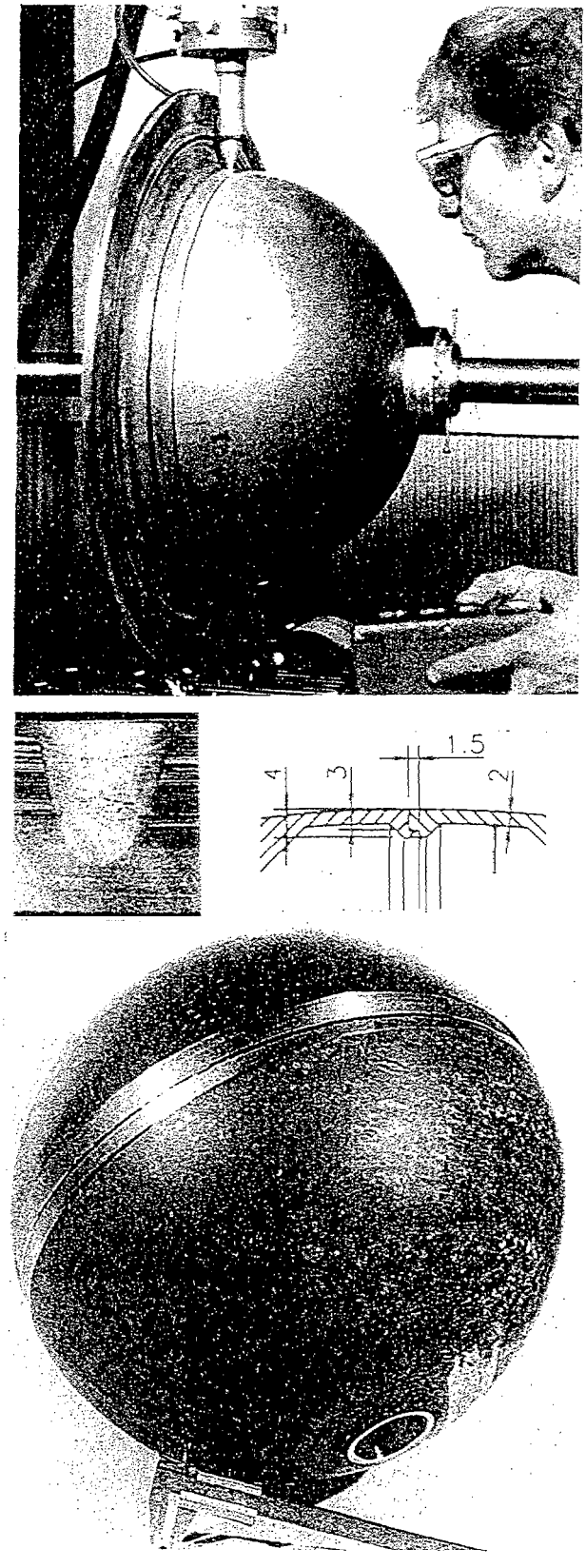

Fig, 29 Spherical reservoir for space applications built of Ti6Al4V (dia. 400 mm), Top: flange of half-shell obtained by superplastic forming being cut at CO2 laser. Centre: Macrograph and joint geometry. Bottom: Two half-shells after welding and cosmetic runs.

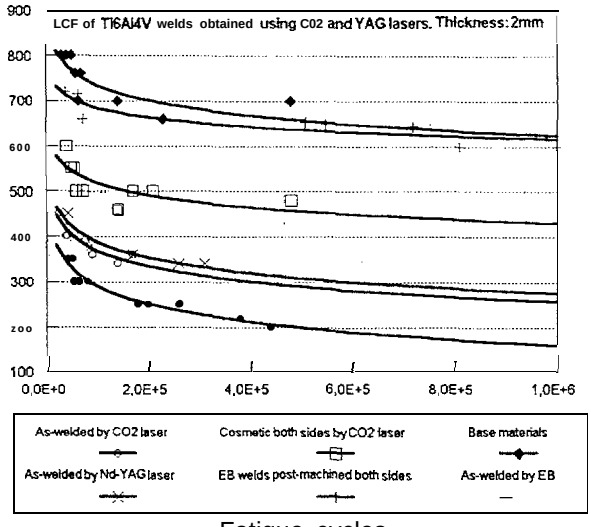

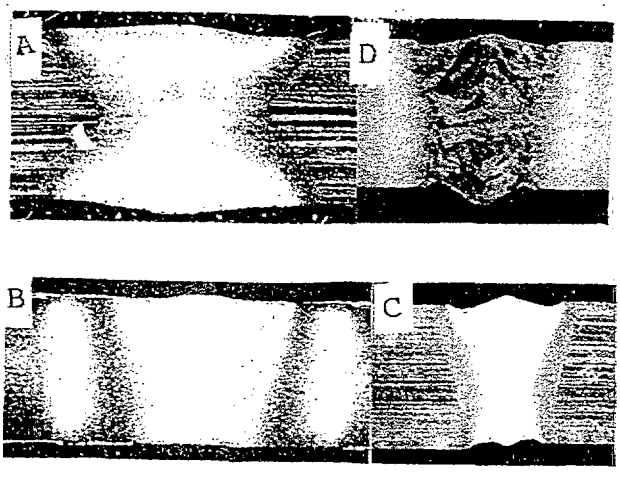

Fig, 30. Fatigue tests on 2-mm thick Ti6A14V welded joints.

The graph curves are (from top down): 2-mm thick base material; EB weld plus machining away of top and root of bead from 4 to 2 mm;
CO_2 laser weld plus cosmetic runs both sides (A); as-welded by YAG laser (B); as-welded by CO_2 laser (C); as-welded by EB (D)..
Fig. 31 shows fatigue tests on 4-mm thick Ti6A14V welded byCO_2 lasers, Top curve: after cosmetic runs on both sides (Fig. 31 E); bottom curve: as-welded (Fig. 3 IF). The bead geometry shows a high influence on fatigue strength; in particular the undercuts and sputterings cause crack initiation. The cosmetic runs on both sides of the weld significantly improve fatigue strength and so are very well suited for structures where surface machining is not possible or allowed, especially sheet metal shells, where smoothness is the prerequisite for good surface aerodynamics.

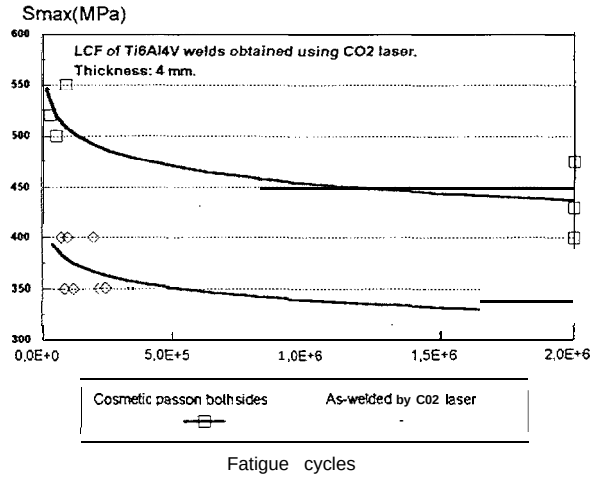

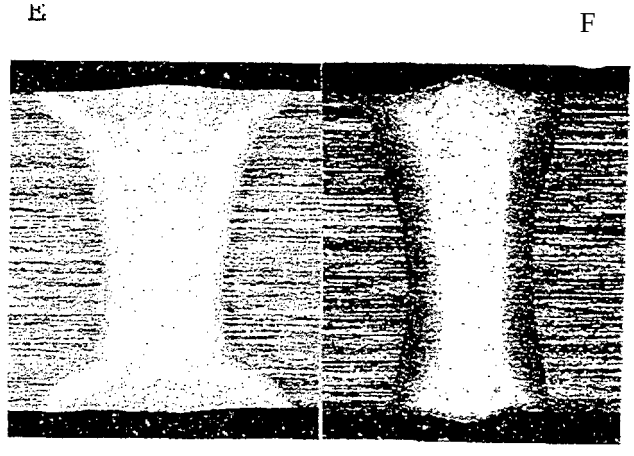

Fig. 31. Fatigue tests on CO_2 laser-welded 4-mm thick Ti6A14Vjoints, with and without cosmetic runs.

6. *CONCLUDING REMARKS*

Even though the BRITE/EURAM projects have the character of basic precompetitive research, the aim of this project was to extend the activity also to provide a demonstration of feasibility on different real industrial components in order to tackle manufacturing problems using laser technology. Further appropriate refinements of the process and systems must be developed to satisfy the technical specifications of the individual components and meet the organisational requirements of individual companies.
While this project was in progress, new. more efficient and less costly laser sources have come on the market. In particular, there has been a big development of Nd-YAG solid-state lasers, and recently the 6-kW average-power laser source has become available for this project. These types of laser source can weld quite large thicknesses, exploiting the flexibility made possible by fibre optics, and hence are able to compete favorably with CO_2 lasers. Both titanium and superalloy structures for new commercial products (e.g., aeroengines) have been conceived in view of their being assembled using laser technology as an additional manufacturing tool.
Until just recently, amortisation of laser systems was based upon mass production of relatively small-sized pieces; today, the welding of lightweight structures having a diameter of 1500 mm produced in small numbers per month is already a reality.

7. REFERENCES

[1] Matthew J. Donachie Jr., Introduction to superalloy, in Matthew J. Donachie, Jr. (Ed,), Superalloys Source Book, ASM, OH (19S4) 3-19

[2] R.P. Jewett and J.A. Halchak, The Use of Alloy 718 in the Space Shuttle Main. Engine, in E.A. Loria (Ed.). Superalloy 718 , 625 and Various Derivatives, TMS (1991) 749-760

[3] William A. Owczararski, Process and metallurgical factors in joining superalloy and other high service temperature materials, in Matthew J. Donachie, Jr. (Ed,), Superalloys Source Book, ASM, OH (1984) 369-400.

[4] A. Lingenfelter, Welding of Inconel Alloy 718: Historical overview, in E. A. Loria (Ed), Superalloy 718 - Metallurgy and Applications, TMS (1989), 673.

[5] S. Gobbi and Li Zhang, High power C02 and Nd:YAG laser welding of Wrought Inconel 718, in M.S.J. Hashmi (Ed) Advances in Materials and Processing Technologies. Dublin (1993), 1225-1238.

[6] Mary McCay et al, Laser Welding Techniques for Alloy 718, in E. A. Loria (Ed), Superaslloys 718,625 and Various Derivatives, TMS (1991) 719-743.

[7] Stephen W, Holcomb and Donald F. Atkins, High-Cycle Fatigue Effects of an Electron-Beam Cosmetic Pass or a Gas Tungsten Overlay on Microfissured Alloy 718, in E.A. Loria (Ed), Superalloy 718 - Metallurgy and Applications, TMS (1989) 467478.

[8] R.G. Thompson et al, The Relationship Between Grain Size and Microfissuring in Alloy 718, Welding Journal, 4 (1985) 91 S-96S.

[9] P. Adam, High Temperature Alloys for Gas Turbines, in D. Coutsouradis et al (Ed). London (1 978)

[10] B. Radhakrishnam and R.G. Thompson, A Model for the Formation and Solidification of Grain Boundary Liquid in the Heat Affected Zone (HAZ) of Welds, Metall. Trans. Vol 23 A. 6 (1992) 1783-1799.

[11] H.J. McQueen, Metal Forming: Industrial, Mechanical Computational and Microstuctural, Journal of Materials ProcessingTechnology, 37 (1993) 3-36.

[12] Unpublished works.

[13] R.G. Thompson et al. The Relationship between Carbon Content. Microstructure and Intergranular Liquation Craking in Cast Nickel Alloy 718. Metal]. Trans. A, Vol 22A. 2 (1991) 557-567.

[14] W, W. Mullins and R.F. Sekerka, Stability of a Planar Interface During Solidification of a Dilute Binary Alloy, Journal of Applied Phisics, Vol. 35 (2), 2 (1964), 444-451.

[15] R.G. Thompson et al, The effect of Heat Treatment on Microfissuring in Alloy 718, Welding journal 11 (1986) 229 S-304S.

[16] Jhon E. Ftin et al, Microstructure and mechanical properties of Alloy 718 Processed by Rapid Solidification, in E. A. Loria (Ed) Superalloys 718, 625 and Various Derivatives. TMS. (1991), 251-260.

[17] Titanium and Titanium Alloys Source Book, in Matthew J. Donachie, Jr. (Ed.), ASM Metals Park, Ohio 44073-1982.

8. A KNOWLEDGMENTS

The above paper has been taken from the results of the project " Laser Welding of Superalloys and of Titanium Alloys " n.4096, contract 91- 0518, developed in the frame of the Basic Research on Industrial and Advanced Material Technologies (BRITE / EURAM IMT programme, supported by the Commission of the European Union, Directorate General XII, N.75 Rue Montoyer, Bruxelles - Belgium.